Synthesis and Characterization of Graphitic Carbon Nitride Supported Tris(Hydroxymethyl)Aminomethanem) G-C_3N_4/ THAM) as Novel Catalyst for the Synthesis of Poly Hydroquinoline and Pyranopyrazole Derivatives

Mohammad taghi bagherian jamnani
Islamic Azad University
Rahimeh Hajinasiri
Islamic Azad University
Hossein Ghafuri (ghafuri@iust.ac.ir)
Iran University of Science and Technology
Zinatossadat Hossaini
Islamic Azad University

Research Article

Keywords: graphitic carbon nitride, tris(hydroxymethyl)aminomethane (THAM), pyranopyrazole, Hantzsch.

Posted Date: October 13th, 2021

DOI: https://doi.org/10.21203/rs.3.rs-958810/v1

Abstract

Here, an impressive heterogeneous catalytic system, graphitic carbon nitride supported tris(hydroxymethyl)aminomethanem) g-C_3N_4/ THAM) is presented. The novel g-C_3N_4/ THAM nanocatalysts was characterized by analyzing methods such as FT-IR, EDX, XRD, TGA, and FESEM. Afterward, the performance of fabricated nanocatalyst g-C_3N_4/ THAM was suitably investigated in multicomponent reactions (MCRs) for the synthesis of 1,4-dihydropyridine and pyranopyrazole derivatives. By optimizing reported nanocatalyst, the corresponding reaction products were obtained with excellent efficiency and then the reversibility process was exanimated. The g-C_3N_4/ THAM nanocatalyst is environmentally friendly and was catalyzed the reactions in the presence of ethanol as a green solvent.

Introduction

Graphitic carbon nitride (g-C_3N_4) this astounding material, is certainly one of the oldest economical and nontoxic polymeric catalyst [1]. The g-C_3N_4 is made easily and large-scale by thermal polymerization (hydrothermal method) from inexpensive precursors such as melamine, dicyandiamide, urea, etc. without the use of organic solvent and is considered a green method [2–5]. The g-C_3N_4 due to its characteristics such as having a small bandgap (2.7 v), non-toxicity, porous structure, high thermal stability, large surface area, remarkable mechanical properties as a catalytic support for many heterogeneous catalytic application processes [6–8]. Due to the special morphology and available surface of polymeric g-C_3N_4, it is extremely easier to modify the structures of g-C_3N_4.As a consequence, The g-C_3N_4 became a hot topic for study,and Its surface can be modified with different functional groups to achieve the desired application.

Many reactions have been done with modified carbon nitride, such as oxygen reduction reaction [9], carbonylation reaction[10], electrooxidation of alcohols[11], photocatalyst [12], and multi-component reactions like the synthesis of imidazole derivatives [13], quinoxaline derivatives [14], and polysubstituted pyridine[15].

Tris (hydroxymethyl) aminomethane (THAM) molecule can be described as consisting of three CH_2OH groups and an NH_2 functional group. The THAM molecule particular structure enriches it with donor-acceptor groups[16] .This structure is a creative and very interesting combination that broadly used in molecular biology, biochemistry and chemistry[17,18]. One of the things that has attracted the attention of chemists to this molecule is its non-toxicity, cost-effectiveness, degradability and biocompatibility of the compound [19].

The use of multicomponent reactions (MCRs) paves the way for us to synthesize complex compounds with more confidence [20]. In many multi-component reactions with the change of one substance new compounds would synthesis. Simple purification of products, mild reaction conditions, and high yields are the benefits of these reactions [21].

Despite their complexity, MCRs have been identified since the beginning of organic chemistry in the nineteenth century[22]. Up to date, more than a dozen MCRs have been developed, many of them named after people. Many basic MCRs, for instance, Passerini[23], Ugi [24], Biginelli[25], Strecker [26], Pictet- Spengler [26], Hantzsch [27], Mannich [28], Kabachnik–Fields [29], and Döbner [30] are named reactions.

Among them, the Hantzsch reaction is one of the oldest, most famous, and challenging multicomponent reactions and it was discovered in 1882 [31,32]. Hantzsch derivatives are one of the significant heterocyclic compounds due to their pharmacology properties such as antitumor [33], calcium channel blockers [34], analgesic [35], and neuroprotective [36] and still is on progress. One-pot condensation of aldehydes, dimedone, ammonium acetate, and ethyl acetoacetate in reflux condition is the classical method of synthesis unsymmetric 1,4-dihydropyridines. This previous method also has some problems such as long reaction time, use of toxic solvents, and low yields that scientists are trying to solve [37,38].

pyranopyrazole are another functional and important compound that is more easily synthesized by MCRs [39]. Due to various properties of pyranopyrazole derivatives such as anticancer[38], anti-inflammatory[40], antimicrobial[41], anti-HIV, and biological activities their synthesis is interesting. Also, many bioactive compounds that have agrochemical and medical activities containing pyranopyrazole ring. Due to these compounds' remarkable properties, scientists are doing their best to synthesis pyranopyrazole derivatives with several methods[42]. The reported methods have disadvantages such as long reaction time, complex and hard work-up process, and also the destructive environment [43].

In this report, we have introduced a new catalyst, g-C_3N_4/ Pr/THAM composite that shown in scheme 1 and used it as novel nanocatalyst in the synthesis of 1,4-dihydropyridine and pyranopyrazole derivatives. Some advantages of using this catalyst are high yields, mild reaction conditions, use of non-toxic solvents, short reaction time, and simple purification. To prepare this nanocatalyst, g-C_3N_4 is synthesized as a substrate and its surface modified with THAM ligand to create a synergistic effect. Mentioned ligand was placed on the substrate surface with 1,3-dibromopropane linker.

Experimental

General

All chemicals were purchased by the Merck Company and used without further purification. The melting points of the prepared derivatives were measured by an electrothermal 9100 apparatus. Al-plates supported by silica gel F254 were used for monitoring reaction progress. The X-ray diffraction (XRD) pattern was obtained using PHILIPS-PW 1800 diffractometer with monochromatized Cu Kα radiation (λ=1.542 Å). Fourier transform infrared (FT-IR) spectra of compounds were performed on a Bruker Tensor27 FT-IR spectrometer. thermal stability of samples was studied by Thermogravimetric analysis (TGA) using the STA504 analyzer system. energy-dispersive X-ray (EDX) spectroscopy for elemental studying of the catalyst was recorded on Oxford Instrument (ZEISS- Sigma VP). Field emission scanning

electron microscopy (FESEM) were carried out on MRIA3 TESCAN-XMU. The purity of the obtained products was confirmed by Varian Inova 500 NMR Spectrometer in DMSO-*d*6.

Synthesis of bulk g-C_3N_4 and g-C_3N_4 nanosheets

The bulk g-C_3N_4 was synthesized by heating melamine with a rate of 2.5 ℃ min^{-1} using a muffle furnace and kept for 2 h at 550 ℃ with the ramp for 4h. After cooling down to ambient temperature, bulk g-C_3N_4 was ground into light yellow color and fine powder. For the preparation of the g-C_3N_4 nanosheets, first 1.0 g bulk g-C_3N_4 was added into 20 mL of H_2SO_4 under stirring for 1 h at 90 ℃. After 5h, 200.0 mL ethanol was added to the mixture and stirred at room temperature yielding a white mixture. The reaction was complete after 2 h. The white precipitate was formed which was separated by simple filtration, then it was washed several times with deionized water, and dried in the oven at 60℃.

Synthesis of sheet g-C_3N_4/Pr/tris(hydroxymethyl)aminomethane composite

In the first step, a mixture of 0.027 g sodium iodide, 0.028 g potassium carbonate, 0.026 g tris(hydroxymethyl)aminomethane, 0.5 ml 1,3-dibromopropane, and 20 ml dry toluene as solvent was added in a round bottom flask and refluxed for 12h. Then, the product was filtered and washed with ethyl acetate.

In the next step, in a round bottom flask, a mixture of the obtained salt product, 0.027 g sodium iodide, g-C_3N_4 (0.1 g), and 20 ml dry toluene was added and refluxed for 12h. Finally, the product was filtered and washed with ethyl acetate and water to remove unreacted materials (scheme 2).

General procedure for the synthesis of 1,4-dihydropyridine derivatives

A mixture of aldehyde (1.0 mmol), ethyl acetoacetate (1.0 mmol), dimedone (1.0 mmol), ammonium acetate (1.0mmol), g-C_3N_4/Pr/ THAM nanocatalyst (20.0 mg), and ethanol (2.0 ml) was added in a round bottom flask and refluxed at 70 ℃. After completion of the reaction, (monitored by TLC), the catalyst was separated by filtration. Eventually, the products were obtained by recrystallization.

General procedure for the synthesis of pyranopyrazole derivatives

A mixture of aldehyde (1.0 mmol), ethyl acetoacetate (1.0 mmol), hydrazine hydrate (1.0 mmol), malononitrile (1.0mmol), g-C_3N_4/Pr/ THAM nanocatalyst (20.0 mg), and ethanol (2.0 ml) was added in a round bottom flask and refluxed at 70 ℃. After completing the reaction (monitored by TLC), the catalyst was separated by filtration. Eventually, to purifying the product was used recrystallization.

Spectral data of selected products

Ethyl-1,4,7,8-tetrahydro-2,7,7-4-(4-chlorophenyl)-5-(6H)-oxoquinolin-3-carboxylate (5b):

IR (KBr): 3445, 3416, 3291, 3222, 2957, 1695, 1612, 1072, 847 cm^{-1}; ^1H NMR (DMSO-d_6, 500 MHz): δ_H = 0.99 (3H, s, CH_3), 1.11 (3H, s, CH_3), 1.12 (3H, t, CH_3), 2.14 - 2.25 (m, 4H,), 2.35 (3H,s, CH_3), 4 (2H,q), 4.83 (1H,s, CH), 7.14 (2H,d), 7.23 (2H,d), 9.1 (1H,s, NH).

6-Amino-4-(4-chlorophenyl)-3-methyl-2,4-dihydropyrano[2,3-c] pyrazole-5-carbonitrile (10b):

IR (KBr):3480,3235,2188,1640,1596 cm^{-1}; ^1H NMR (DMSO-d_6, 500 MHz): δ_H (ppm) = 1.79 (3H, s, CH_3), 4.63 (1H, s, CH), 6.91 (2H, s, NH_2), 7.192–7.20 (2H, d, H-aromatic), 7.37–7.38 (d, 2H, H-aromatic), 12.12 (1H, s, NH).

Results And Discussion

To investigate the surface functionalization g-C_3N_4 substrate characterized by Fourier transform infrared (FT-IR), energy-dispersive X-ray (EDX) spectroscopy indicates the type of elements present in the g-C_3N_4/Pr/ THAM nanocatalyst. X-ray diffraction (XRD) pattern is shown to investigate the crystal structure of the compound and the field emission scanning electron microscope (FESEM) analysis indicates the morphology of the synthesized catalyst surface. Finally, the heat resistance of the desired compound is characterized by Thermogravimetric analysis (TGA).

FT-IR spectroscopy

According to the spectrum presented in Figure 1, a broad peak has appeared in the range of 3000-3300 cm^{-1}, which is related to the stretching vibration of NH bonds; the peak width can be assigned to NH groups involved in the hydrogen bond or the existence of the OH group. The stretching vibrational peak C =N is observed at 1602 cm^{-1}. Peaks 1303 and 1082 cm^{-1} are attributed to the tensile vibration of C-N bonds formed between triazine and N-H groups, and the stretching vibration of C-N bonds in the ring in 1448 and 1379 cm^{-1} is easily visible. Also, the peak is 786 cm^{-1} due to the vibration of tri-s-triazine units. The presence of C-H stretching peaks (2800-3000 cm^{-1}) confirms the synthesis of the desired composite.

EDS analysis

In this section, we will go to the EDS spectrum to confirm the synthesis of the g-C_3N_4 /THAM nanocatalyst compound. As shown in Figures 2, presence elements such as C, N, O confirms the synthesis of g-C_3N_4 / THAM nanocatalyst. Very small amounts of sodium, potassium and iodine are observed in the analysis, all of which are related to substances that added to the reaction to modify the surface carbon dioxide. Due to many elements and their disintegration, the names of the elements are not mentioned in the device's intermediate diagram; they are listed in the quantitative table shape.

XRD analysis

The structure of the g-C_3N_4/Pr/ THAM nanocatalyst was characterized using by XRD pattern. As observed in Figure 3, the broad and intense reflection peaks at 2θ= 27.4 were assigned to the reflection

peak of graphitic carbon nitride with Card No. JCPDS 87-1526. The new couriers have corresponded to the surface modification and nanocatalyst synthesis.

FE-SEM analysis

FESEM analysis was used to study the morphology and particle size distribution of the synthesized nanocomposite. Figure 4(a-d) has demonstrated images of nano-sheets g-C_3N_4 and nano-sheets g- C_3N_4/ Pr/THAM nanocatalyst by FE-SEM studies. As expected, FE-SEM images of graphitic carbon nitride (a,b) are smooth and are almost neatly linked and placed on each other due to being graphitic. In nano-sheets g-C_3N_4/ Pr/THAM nanocatalyst images (c,d), g-C_3N_4 plates are not smooth and have particles on them that exhibited the synthesis of the nanocomposite. Also, carbon nitride nano-sheets have become irregular.

TGA analysis

These observations also agree with the thermogravimetric analysis (TGA). Figure 5 shows the thermal stability of synthesized graphitic carbon nitride/ tris(hydroxymethyl)aminomethane composite which was carried out by TGA. The resulting catalyst as evidenced by TGA has displays high-temperature resistance up to approximately 400 °C. The mass-loss curve presents an inflection point at 400 °C. From 400°C, the diagram exhibits a gentle slope which is probably due to the decomposition of the composite before entering a nearly sharp slope being attributed to the thermal decomposition of carbon nitride.

Catalyst application of the g-C_3N_4/Pr/ THAM nanocatalyst in MCRs

The catalytic activity of the g-C_3N_4/Pr/ THAM nanocatalyst was studied in two MCRs for the synthesis of 1,4-dihydropyridine and pyranopyrazole derivatives to obtain the highest performance. To achieve the best result, different experimental conditions such as temperature, solvent, and amount of catalyst must be examined. To optimize the reaction conditions and performance evaluation of the g-C_3N_4/Pr/THAM nanocatalyst in Hantzsch reaction for the synthesis of 1,4-dihydropyridine derivatives, a one-pot four components reaction of chlorobenzaldehyde (1 mmol), ethyl acetoacetate (1 mmol), dimedone (1 mmol), and ammonium acetate (1 mmol) were investigated as a model reaction. Also, for the synthesis of pyranopyrazole derivatives a four-component reaction ethyl acetoacetate (1 mmol), hydrazine hydrate (1 mmol),4- chlorobenzaldehyde (1 mmol), and malononitrile (1 mmol) in ethanol was considered as the model reaction. Both model reactions showed almost the same behavior. One of the crucial factors in multicomponent reactions is solvent selection due to the different yields of each catalyst in different solvents. therefore, we have examined different solvents (protic and aprotic) to observe the effect. First, optimization experiments were conducted in ethanol, methanol, acetonitrile, DCM, DMF, DMSO, THF, toluene, water, ethanol/water (3:1), methanol/water (3:1), and solvent-free conditions as green conditions in both model reaction and the best efficiency were obtained in ethanol (Table 1, entries 1). Among these solvents, just MeOH, DCM, and ACN gave the intended product for 92, 60, and 66% yield, respectively (Table 1, Entries 2-4). Protic solvents have shown great progress in model reactions in comparison to

aprotic solvents. In aprotic solvents, the intended product has not been seen in TLC even after 1h. Thus, we have desired to use protic solvents more than aprotic solvents. Unfortunately, model reactions showed no intended product in TLC in water as solvent (Table 1, entry 9). The insolubility of organic compounds in water could be the reason for this event. Therefore, we have used the combination of water and ethanol (Table 1, entries 10-11). The results showed that the existence of water would decrease the yields. We also tried model reactions in solvent-free conditions. In these conditions, the intended product has not been seen in TLC even after 1h. After concluding the results, ethanol was the best solvent among the others and was selected as the constant solvent for further studies.

The subsequent model reaction was performed without catalyst and in the presence of ethanol, the yield of this MCRs was not considerable (Table 1, entries 14). Another critical factor in multicomponent reactions is the amount of catalyst in the reaction. By adding the g-C_3N_4/Pr/ THAM nanocatalyst to the model reaction in the presence of a solvent, the efficiency increased dramatically and the yield was reached about 91%. Thus, we have examined the different amounts of the catalyst to find the optimum amount, and the results have shown in Table 1. Hence, we have added 0.01 g of catalyst to the reaction mixture. The TLC monitoring showed that the intended product is produced (Table 1, Entry 15). For optimizing catalyst amount, we have increased the amount by 30 mg. As a result, it showed that the amount of catalyst upper 0.02 g does not affect the yield of the intended product. (Table 1, Entry 18). Accordingly, it was observed that 0.02g nanocatalyst is sufficient to conduct this MCRs.

Table 1. Optimizing the reaction conditions in the synthesis of 1,4-dihydropyridine[a] and pyranopyrazole[b] derivatives

Entry	Solvent	Catalyst amount (g)	Time (min)	Yield[(a)] (%)	Yield[(b)] (%)
1	EtOH	0.02	15	90	91
2	MeOH	0.02	15	87	85
3	MeCN	0.02	15	68	63
4	DCM	0.02	15	53	50
5	DMF	0.02	60	_	_
6	DMSO	0.02	60	_	_
7	THF	0.02	60	_	_
8	Toluene	0.02	60	_	_
9	H_2O	0.02	60	_	_
10	EtOH/H_2O (3:1)	0.02	15	75	73
11	EtOH/H_2O (3:1)	0.02	15	68	64
12	_	0.02	60	_	_
13	_	0.02	60	_	_
14	EtOH	_	60	_	_
15	EtOH	0.01	15	53	50
16	EtOH	0.015	15	73	71
17	**EtOH**	**0.02**	**15**	**90**	**91**
18	EtOH	0.03	15	66	64

(a) Reaction conditions: chlorobenzaldehyde (1 mmol), ethyl acetoacetate (1 mmol), dimedone (1 mmol), and ammonium acetate (1 mmol), catalyst (0.01-0.03 g), the yields relate to the isolated product.

(b) Reaction of ethyl acetoacetate (1 mmol), hydrazine hydrate (1 mmol), 4- chlorobenzaldehyde (1 mmol) and malononitrile (1 mmol), catalyst (0.01-0.03 g), the yields relate to the isolated product.

After the optimization process, the generality of the procedure was evaluated by the reaction of different aromatic aldehydes with different types of electron-donating and electron-withdrawing groups. As observed in Table 2 and 3, all desired product was obtained with high yields in short reaction times. After optimizing the reaction conditions, we investigated the limitation and generality of the presented procedure using different aromatic aldehydes (Table 2 and 3).

Table 2. The synthesis of 1,4-dihydropyridine derivatives in optimized condition using g-C_3N_4/Pr/ THAM nanocatalyst.

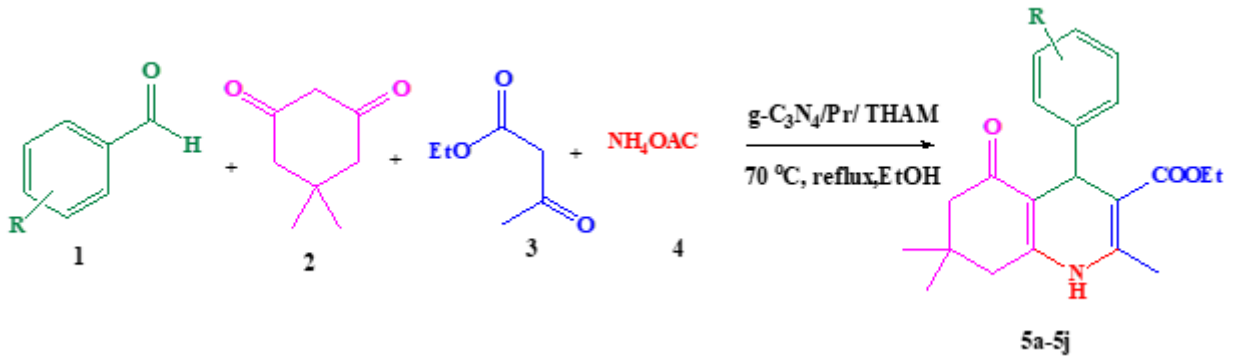

Entry	R	Products	Time (min)	Mp (°C)		Yield[a] (%)
				Observed	Literature	
1	H	5a	15	201-203	203-204[44]	90
2	4-Cl	5b	15	245-246	245-246[45]	96
3	3-NO_2	5c	30	182-183	180-183[46]	89
4	4-OH	5d	25	231-233	231-233[46]	87
5	2-Cl	5e	15	200-202	202-204[47]	95
6	4-Me	5f	25	259-261	259-262[48]	86
7	4-NO_2	5g	20	241-243	241-243[49]	90
8	4-OMe	5h	25	256-258	258-260[50]	87
9	2,4-Cl	5i	35	241-243	240-242[51]	94
10	3-OH	5j	30	232-233	230-232[52]	89

[a] The yields relate to the isolated product.

Table 3. The synthesis of pyranopyrazole derivatives in optimized condition using the g-C_3N_4/Pr/ THAM nanocatalyst.

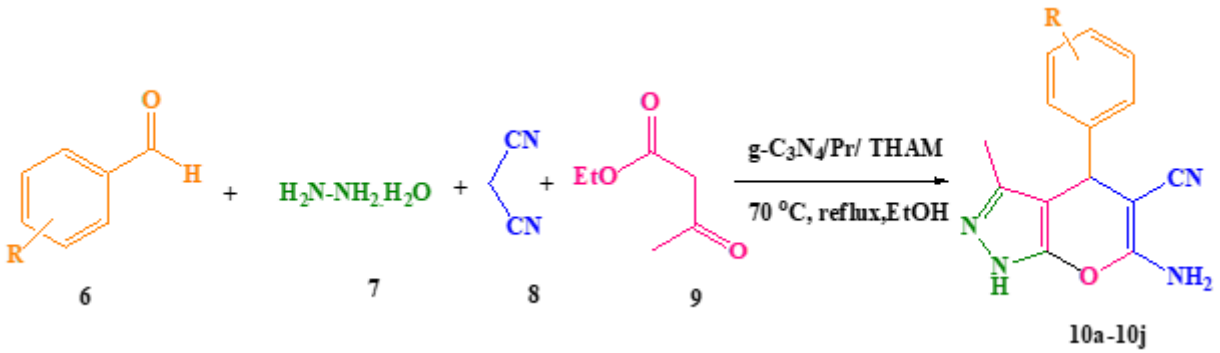

Entry	R	Products	Time (min)	MP (°C)		Yield[a] (%)
				Observed	Literature	
1	H	10a	20	244-246	[53]243-245	91
2	4-Cl	10b	20	231-233	[43]230-232	95
3	4-NO_2	10c	25	250-252	[54]250-251	88
4	2,4-Cl	10d	40	234-236	[55]234-236	92
5	4-OH	10e	30	223-224	[55]223-224	93
6	4-Me	10f	30	176-177	[55]177-178	91
7	3-NO_2	10g	35	213-215	[55]213-216	93
8	2-Cl	10h	20	255-257	[55]245-246	93
9	4-MeO	10i	30	176-177	[55]177-178	87
10	4-Br	10j	35	180-182	[56]179-181	90

[a] The yields relate to the isolated product.

Suggested mechanism for synthesis of pyranopyrazole and 1,4-dihydropyridine derivatives

The characteristics of g-C_3N_4/Pr/THAM nanocomposite as a multifunctional catalyst was utilized for the synthesis pyrano[2,3-c]pyrazol and 1,4-dihydropyridine derivatives.

The Hantzsch reaction widely used for direct synthesis of 1,4-dihydropyridine (DHPs) derivatives. Based on previous studies [57,58], we propose the following mechanism for the synthesis of 1,4-dihydropyridine derivatives. We know that the surface of our g-C_3N_4/Pr/THAM catalyst plays an important role for the synthesis of desired derivatives. 1,4-dihydropyridine derivatives are synthesized by two slightly different methods. In the first method which presented in Scheme 3, the critical intermediate (I) formed through Knoevenagel condensation of benzaldehyde and dimedone in the presence of g-C_3N_4/Pr/THAM. On the other hand, the nucleophilic attack of the nitrogen of the ammonium acetate and the condensation of ethyl acetoacetate and ammonium acetate generated the intermediate (II). The next step involves Michael addition of (II) to (I), ring closing, and water elimination produced 1,4-dihydropyridine derivatives. But there is another mechanism for this reaction, In the second method, the reaction between dimedone and ammonium acetate in the presence of catalyst would obtain intermediate (III). The reaction between ethyl acetoacetate and aldehyde would obtain intermediate (IV). Eventually, by the reaction of two intermediates, the corresponding product would obtain and the g-C_3N_4/Pr/ THAM nanocatalyst was returned to reaction cycle. Also, the essential role of the catalyst is shown.

To form the pyranopyrazole derivatives, the g-C_3N_4/Pr/THAM nanocomposite as a bifunctional catalyst was utilized. According to reported articles [43,57] ,we have proposed a plausible reaction mechanism for the preparation of pyranopyrazole derivatives which is outlined in Scheme 4. First, the carbonyl groups were subjected to the nucleophilic attack of hydrazine hydrate with two nucleophilic sites. At this stage, by removing water and ethanol molecules respectively and also tautomerization intermediate (I) is formed. On the other hand, intermediate (II) was produced via Knoevenagel condensation reaction and with loss of H_2O between catalyst-activated aromatic aldehyde and malononitrile. In the second stage, two intermediate pyrazolone ring and 2-phenylidenemalononitrile catalyzed with g-C_3N_4/Pr/ THAM compound and produced intermediate (III) and (IV). These compounds are formed by the reactions Michael addition, 6-exo-dig cyclization respectively. In the last step, by proton transfer and tautomerization of molecule (IV), the desired pyranopyrazole derivatives were obtained. Then g-C_3N_4/Pr/THAM nanocatalyst was returned to the reaction cycle to reuse.

Reusability

Reusability is one of the most important factors in any catalyst system, which highlights them as an efficient system due to time savings and economic benefits. The reusability of this synthesized catalyst was investigated in two MCRs. Initially, the heterogeneous catalyst was separated from the reaction mixture with filter paper. Then, it was washed several times with water and ethanol and dried in an oven at 80 ° C. It was observed that the catalyst can be reused at least five times without significantly reducing its activity (Figure 6).

Conclusion

In this paper, we have successfully synthesized g-C_3N_4/ tris(hydroxymethyl)aminomethane that have –OH functions. Next, we used this catalyst in two different multicomponent reactions to investigate the catalytic properties in various reactions. As shown, the yields of the pure products either in the Hantzsch reaction or in the synthesis of pyranopyrazole derivatives were excellent and high. Also, the intended products have been purified by simple recrystallization. The advantages of using this catalyst in organic reactions are high yield, non-toxic, easy separation, and reusability.

Declarations

ACKNOWLEDGMENTS

We are grateful for the financial support from The Research Council of Iran University of Science and Technology (IUST), Tehran, Iran.

References

1. Uekert, T., Kasap, H. & Reisner, E. Photoreforming of nonrecyclable plastic waste over a carbon nitride/nickel phosphide catalyst. *J. Am. Chem. Soc.* **141**, 15201-15210 .(2019)
2. Jiang, J. *et al.* Dependence of electronic structure of g-C_3N_4 on the layer number of its nanosheets: a study by Raman spectroscopy coupled with first-principles calculations. *Carbon* **80**, 213-221.(2014)
3. Zhang, H. & Yu, A. Photophysics and photocatalysis of carbon nitride synthesized at different temperatures. *J. Phys. Chem. C* **118**, 11628-11635.(2014)
4. Liu, J., Zhang, T., Wang, Z., Dawson, G. & Chen, W. Simple pyrolysis of urea into graphitic carbon nitride with recyclable adsorption and photocatalytic activity. ***J. Mater. Chem.*** **21**, 14398-14401. (2011)
5. Yuan, Y.-P. *et al.* Large impact of heating time on physical properties and photocatalytic H_2 production of g-C_3N_4 nanosheets synthesized through urea polymerization in Ar atmosphere. *Int. J. Hydrog. Energy* **38,** 13159-1316 (2013).
6. Stroyuk, O. *et al.* Spectral and photophysical properties of size-selected ZnO nanocrystals coupled to single-layer carbon nitride sheets. *FlatChem* **2**, 38-48 (2017).
7. Ye, S., Wang, R., Wu, M.-Z. & Yuan, Y.-P. A review on g-C_3N_4 for photocatalytic water splitting and CO_2 reduction. *Appl. Surf. Sci.* **358**, 15-2 (2015).
8. Ayodhya, D. & Veerabhadram, G. Influence of g-C_3N_4 and g-C_3N_4 nanosheets supported CuS coupled system with effect of pH on the catalytic activity of 4-NP reduction using $NaBH_4$. *FlatChem* **14**, 100088 (2019).
9. Yu, J. *et al.* Cobalt Oxide and Cobalt-Graphitic Carbon Core–Shell Based Catalysts with Remarkably High Oxygen Reduction Reaction Activity. *Adv. Sci.* **3**, 1600060 (2016).

10. Lu, P., Chen, W. & Lu, W. Solar photothermal catalytic effect promotes carbonylation reaction based on palladium doped g-C_3N_4 catalyst. *Mater. Res. Bull.* **137**, 111194 (2021).
11. Qian, H., Chen, S., Fu, Y. & Wang, X. Platinum–palladium bimetallic nanoparticles on graphitic carbon nitride modified carbon black: a highly electroactive and durable catalyst for electrooxidation of alcohols. *J. Power Sources* **300**, 41-48 (2015).
12. Wu, M., Yan, J. M., Tang, X. n., Zhao, M. & Jiang, Q. Synthesis of potassium-modified graphitic carbon nitride with high photocatalytic activity for hydrogen evolution. *ChemSusChem* **7**, 2654-2658 (2014).
13. Ahooie, T. S., Azizi, N., Yavari, I. & Hashemi, M. M. Magnetically separable and recyclable g-C_3N_4 nanocomposite catalyzed one-pot synthesis of substituted imidazoles. *J. Iran. Chem. Soc.* **15**, 855-862 (2018).
14. Rashidizadeh, A. & Ghafuri, H. g-C_3N_4/Ni Nanocomposite: An Efficient and Eco-Friendly Recyclable Catalyst for the Synthesis of Quinoxalines. *Multidisciplinary Digital Publishing Institute Proceedings* **9(1)**, 49 (2019).
15. Edrisi, M. & Azizi, N. Sulfonic acid-functionalized graphitic carbon nitride composite: a novel and reusable catalyst for the one-pot synthesis of polysubstituted pyridine in water under sonication. *J. Iran. Chem. Soc.* **17**, 901-910 (2020).
16. Niya, H. F., Hazeri, N., Fatahpour, M. & Maghsoodlou, M. T. Fe_3O_4@THAM-piperazine: a novel and highly reusable nanocatalyst for one-pot synthesis of 1, 8-dioxo-octahydro-xanthenes and benzopyrans. *Res. Chem. Intermed.* **46**, 3651-3666 (2020).
17. Missina, J. M. *et al.* Accessing decavanadate chemistry with tris (hydroxymethyl) aminomethane, and evaluation of methylene blue bleaching. *Polyhedron* **180**, 114414 (2020).
18. El-Dissouky, A. *et al.* X-ray crystal structure, spectroscopic and DFT computational studies of H-bonded charge transfer complexes of tris (hydroxymethyl) aminomethane (THAM) with chloranilic acid (CLA). *J. Mol. Struct.* **1200**, 127066 (2020).
19. Kudale, A. S. *et al.* One-pot three-component synthesis and photophysical properties of highly fluorescent novel 4-alkyl-3-aryl-2, 6-dicyanoanilines by using tris (hydroxymethyl) aminomethane as a catalyst. *Chem. Data Collect.* **19**, 100172 (2019).
20. Wu, H., Wang, Z. & Tao, L. The Hantzsch reaction in polymer chemistry: synthesis and tentative application. *Polym. Chem.* **8**, 290-7296 (2017).
21. Nunes, P. S. G., Vidal, H. D. A. & Corrêa, A. G. Recent advances in catalytic enantioselective multicomponent reactions. *Org. Biomol. Chem.* **18**, 7751-7773 (2020).
22. Kakuchi, R. The dawn of polymer chemistry based on multicomponent reactions. *Polym. J.* **51**, 945-953 (2019).
23. Passerini, M. & Simone, L. Sopra gli isonitrili (I). Composto del p-isonitril-azobenzolo con acetone ed acido acetico. *Gazz. Chim. Ital* **51**, 126-129 (1921).

24. Dömling, A. & Ugi, I. Multicomponent reactions with isocyanides. *Angew. Chem. Int. Ed.* **39**, 3168-3210 (2000).
25. de Fátima, Â. *et al.* A mini-review on Biginelli adducts with notable pharmacological properties. *J. Adv. Res.* **6**, 363-373 (2015).
26. Duthaler, R. O. Recent developments in the stereoselective synthesis of α-aminoacids. *Tetrahedron* **50**, 1539-1650 (1994).
27. Hantzsch, A. Condensationsprodukte aus Aldehydammoniak und ketonartigen Verbindungen. *Chem. Ber.* **14**, 1637-1638 (1881).
28. Bandar, J. S., Barthelme, A., Mazori, A. Y. & Lambert, T. H. Structure–activity relationship studies of cyclopropenimines as enantioselective Bronsted base catalysts. *Chem. Sci.* **6**, 1537-1547 (2015).
29. Keglevich, G. & Bálint, E. The Kabachnik–Fields reaction: Mechanism and synthetic use. *Molecules* **17**, 12821-12835 (2012).
30. Kakuchi, R. Multicomponent reactions in polymer synthesis. *Angew. Chem. Int. Ed.* **53**, 46-48 (2014).
31. Cheng, X., Goddard, R., Buth, G. & List, B. Direct catalytic asymmetric three-component Kabachnik–Fields reaction. *Angew. Chem. Int. Ed.* **47**, 5079-5081 (2008).
32. Qiu, S. *et al.* Highly selective colorimetric bacteria sensing based on protein-capped nanoparticles. *Analyst* **140**, 1149-1154 (2015).
33. Mollazadeh, S., Sahebkar, A., Kalalinia, F., Behravan, J. & Hadizadeh, F. Synthesis, in silico and in vitro studies of new 1, 4-dihydropiridine derivatives for antitumor and P-glycoprotein inhibitory activity. *Bioorg. Chem.* **91**, 103156 (2019).
34. Mojarrad, J. S., Zamani, Z., Nazemiyeh, H., Ghasemi, S. & Asgari, D. Synthesis of novel 1, 4-dihydropyridine derivatives bearing biphenyl-2'-tetrazole substitution as potential dual angiotensin II receptors and calcium channel blockers. *Adv. Pharm. Bull.* **1**, 1 (2011).
35. Indumathi, S., Karthikeyan, R., Nasser, A. J. A., Idhayadhulla, A. & Kumar, R. S. Anticonvulsant, analgesic and anti-inflammatory activities of some novel pyrrole and 1, 4-dihydropyridine derivatives. *J. Chem. Pharm. Res* **7**, 434-440 (2015).
36. Kasza, Á. *et al.* Dihydropyridine derivatives modulate heat shock responses and have a neuroprotective effect in a transgenic mouse model of Alzheimer's disease. *J. Alzheimer's Dis.* **53**, 557-571 (2016).
37. Abdella, A. M., Abdelmoniem, A. M., Abdelhamid, I. A. & Elwahy, A. H. Synthesis of heterocyclic compounds via Michael and Hantzsch reactions. *J. Heterocycl. Chem.* **57**, 1476-1523 (2020).
38. Sharma, A., Chowdhury, R., Dash, S., Pallavi, B. & Shukla, P. Fast microwave assisted synthesis of pyranopyrazole derivatives as new anticancer agents. *Curr. Microw. Chem.* **3**, 78-84 (2016).
39. Khazaei, A., Zolfigol, M. A., Karimitabar, F., Nikokar, I. & Moosavi-Zare, A. R. N, 2-Dibromo-6-chloro-3, 4-dihydro-2 H-benzo [e][1, 2, 4] thiadiazine-7-sulfonamide 1, 1-dioxide: an efficient and homogeneous catalyst for one-pot synthesis of 4 H-pyran, pyranopyrazole and pyrazolo [1, 2-b] phthalazine derivatives under aqueous media. *RSC adv.* **5**, 71402-71412 (2015).

40. Ismail, M. M., Khalifa, N. M., Fahmy, H. H., Nossier, E. S. & Abdulla, M. M. Design, Docking, and Synthesis of Some New Pyrazoline and Pyranopyrazole Derivatives as Anti-inflammatory Agents. *J. Heterocycl. Chem.* **51**, 450-458 (2014).
41. Reddy, G. M., Garcia, J. R., Zyryanov, G. V., Sravya, G. & Reddy, N. B. Pyranopyrazoles as efficient antimicrobial agents: green, one pot and multicomponent approach. *Bioorg. Chem.* **82**, 324-331 (2019).
42. Mamaghani, M. & Hossein Nia, R. A review on the recent multicomponent synthesis of pyranopyrazoles. *Polycycl. Aromat. Compd.* **41**, 223-291 (2021).
43. Hassanzadeh-Afruzi, F., Dogari, H., Esmailzadeh, F. & Maleki, A. Magnetized melamine-modified polyacrylonitrile (PAN@melamine/Fe_3O_4) organometallic nanomaterial: Preparation, characterization, and application as a multifunctional catalyst in the synthesis of bioactive dihydropyrano [2, 3-c] pyrazole and 2-amino-3-cyano 4H-pyran derivatives. *Appl Organomet Chem* **35(10)**, e6363 (2021).
44. Mosaddegh, E. & Hassankhani, A. One-pot synthesis of polyhydropyridine derivatives via Hantzsch four component condensation in water medium: Use of a recyclable Lewis acid [$Ce(SO_4)_2.4H_2O$] catalyst. *Bull. Chem. Soc. Ethiop.* **26**, 461-465 (2012).
45. Ghasemzadeh, M. A. & Safaei-Ghomi, J. An efficient, one-pot synthesis of polyfunctionalised dihydropyridines catalysed by AgI nanoparticles. *J. Chem. Res.* **38**, 313-316 (2014).
46. Zare, E. & Rafiee, Z. Magnetic chitosan supported covalent organic framework/copper nanocomposite as an efficient and recoverable catalyst for the unsymmetrical hantzsch reaction. *J. Taiwan Inst. Chem. Eng.* **116**, 205-214 (2020).
47. Goli-Jolodar, O., Shirini, F. & Seddighi, M. Introduction of a novel nanosized N-sulfonated Brönsted acidic catalyst for the promotion of the synthesis of polyhydroquinoline derivatives via Hantzsch condensation under solvent-free conditions. *RSC adv.* **6**, 26026-26037 (2016).
48. Khazaei, A. *et al.* Synthesis of hexahydroquinolines using the new ionic liquid sulfonic acid functionalized pyridinium chloride as a catalyst. *Chinese J. Catal.* **34**, 1936-1944 (2013).
49. Tekale, S. U., Pagore, V. P., Kauthale, S. S. & Pawar, R. P. La_2O_3/TFE: An efficient system for room temperature synthesis of Hantzsch polyhydroquinolines. *Chin. Chem. Lett.* **25**, 1149-1152 (2014).
50. Harale, R. R., Shitre, P. V., Sathe, B. R. & Shingare, M. S. Visible light motivated synthesis of polyhydroquinoline derivatives using CdS nanowires. *Res. Chem. Intermed.* **43**, 3237-3249 (2017).
51. Maleki, B. *et al.* One-Pot Synthesis of 1,4-Dihydropyridine Derivatives Catalyzed by Silica-Coated Magnetic $NiFe_2O_4$ Nanoparticles-Supported $H_{14}[NaP_5W_{30}O_{110}]$. *Russ. J. Gen. Chem.* **87**, 2922-2929 (2017).
52. Ghorbani-Choghamarani, A., Mohammadi, M., Tamoradi, T. & Ghadermazi, M. Covalent immobilization of Co complex on the surface of SBA-15: Green, novel and efficient catalyst for the oxidation of sulfides and synthesis of polyhydroquinoline derivatives in green condition. *Polyhedron* **158**, 25-35 (2017).

53. Saha, A., Payra, S. & Banerjee, S. One-pot multicomponent synthesis of highly functionalized bio-active pyrano [2, 3-c] pyrazole and benzylpyrazolyl coumarin derivatives using ZrO_2 nanoparticles as a reusable catalyst. *Green Chem.* **17**, 2859-2866 (2015).
54. Shahbazi, S., Ghasemzadeh, M. A., Shakib, P., Zolfaghari, M. R. & Bahmani, M. Synthesis and antimicrobial study of 1, 4-dihydropyrano [2, 3-c] pyrazole derivatives in the presence of amino-functionalized silica-coated cobalt oxide nanostructures as catalyst. *Polyhedron* **170**, 172-179 (2019).
55. Ghafuri, H., Kazemnezhad Leili, M. & Esmaili Zand, H. R. Copper-immobilized ionic liquid as an alternative to organic solvents in the one-pot synthesis of bioactive dihydropyrano [2, 3-c] pyrazole derivatives. *Appl. Organomet. Chem* .**34**, e5757 (2020).
56. Safaei-Ghomi, J., Shahbazi-Alavi, H. & Heidari-Baghbahadorani, E. $ZnFe_2O_4$ nanoparticles as a robust and reusable magnetically catalyst in the four component synthesis of [(5-hydroxy-3-methyl-1H-pyrazol-4yl)(phenyl) methyl] propanedinitriles and substituted 6-amino-pyrano [2, 3-c] pyrazoles. *J. Chem. Res.* **39**, 410-413 (2015).
57. Karami, S., Dekamin, M. G., Valiey, E. & Shakib, P. DABA MNPs: A new and efficient magnetic bifunctional nanocatalyst for the green synthesis of biologically active pyrano [2, 3-c] pyrazole and benzylpyrazolyl coumarin derivatives. *New J. Chem.* **44**, 13952-13961 (2020).
58. Maleki, A., Hassanzadeh-Afruzi, F., Varzi, Z. & Esmaeili, M. S. Magnetic dextrin nanobiomaterial: an organic-inorganic hybrid catalyst for the synthesis of biologically active polyhydroquinoline derivatives by asymmetric Hantzsch reaction. *Mater. Sci. Eng. C* **109**, 110502(2020).

Figures

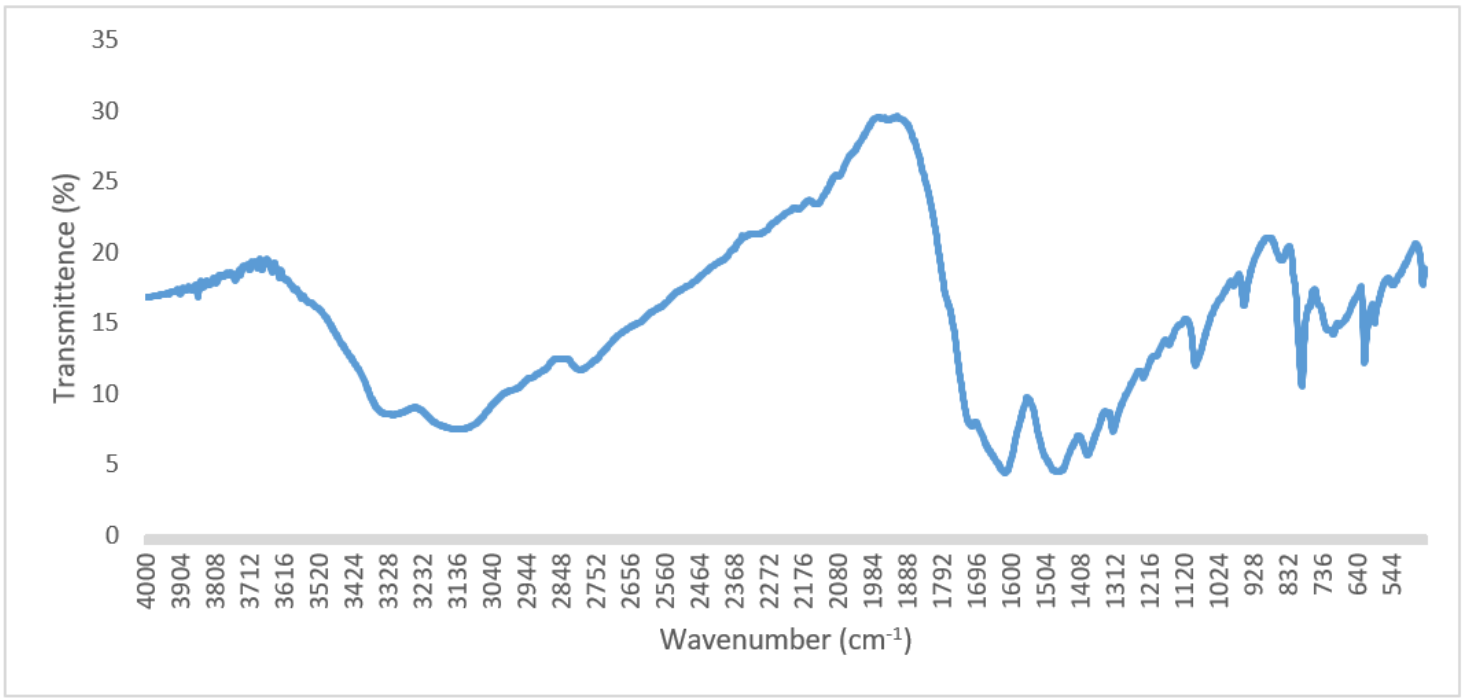

Figure 1

FT-IR spectra of g-C3N4/Pr/ THAM nanocatalyst

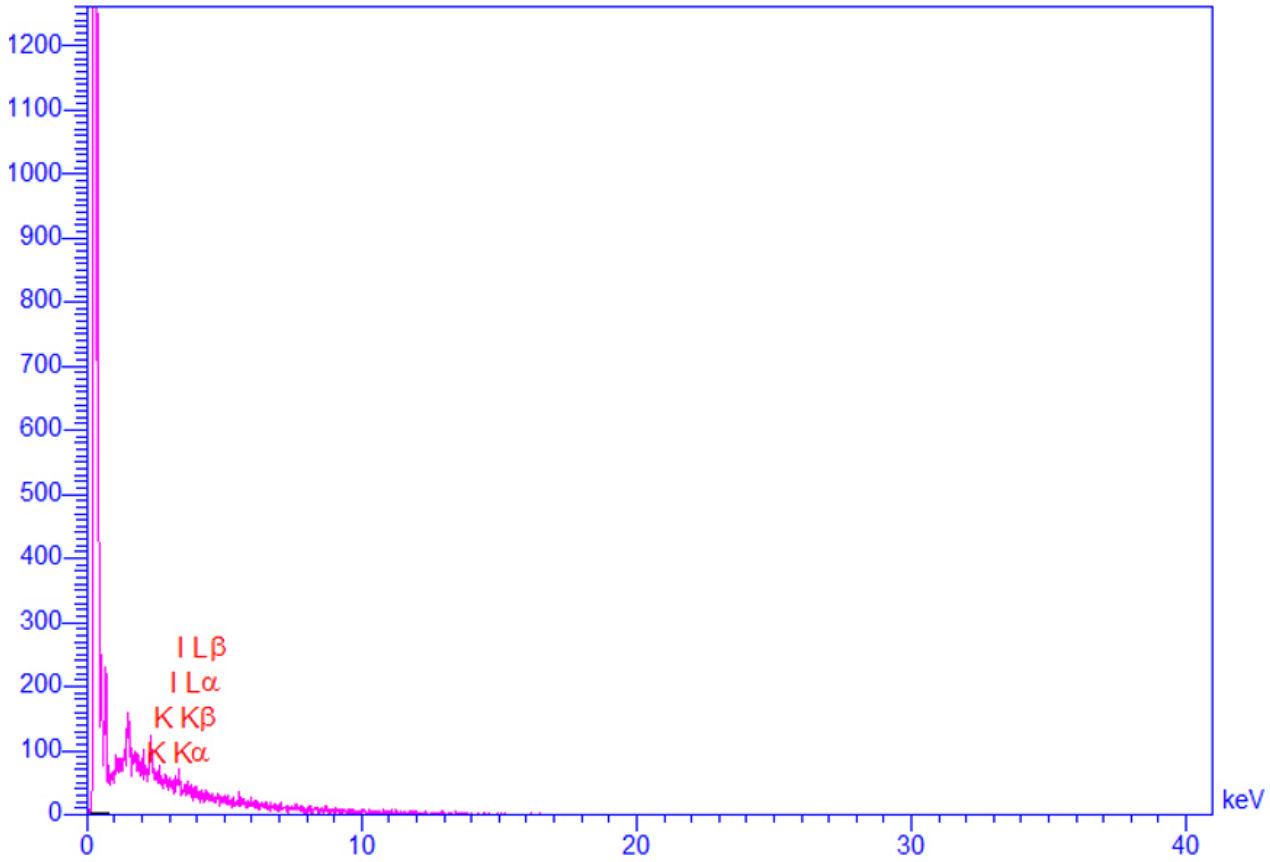

Quantitative Results

Elt	Line	Int	Error	K	Kr	W%	A%	ZAF	Formula	Ox%	Pk/Bg	Class	LConf	HConf	Cat#
C	Ka	1841.4	44.4689	0.5871	0.1674	28.59	32.23	0.5855		0.00	94.95	A	28.17	29.01	0.00
N	Ka	964.8	44.4689	0.3827	0.1091	62.02	59.96	0.1758		0.00	344.14	A	60.77	63.28	0.00
O	Ka	181.8	44.4689	0.0245	0.0070	9.12	7.72	0.0767		0.00	33.54	A	8.70	9.55	0.00
Na	Ka	30.6	44.4689	0.0014	0.0004	0.11	0.07	0.3466		0.00	3.10	B	0.10	0.12	0.00
K	Ka	30.5	1.3120	0.0018	0.0005	0.06	0.02	0.8597		0.00	2.88	B	0.05	0.07	0.00
I	La	14.7	1.3120	0.0025	0.0007	0.09	0.01	0.7493		0.00	2.48	B	0.08	0.11	0.00
				1.0000	0.2851	100.00	100.00			0.00					0.00

Figure 2

EDX spectrum of g-C3N4/ THAM nanocatalyst.

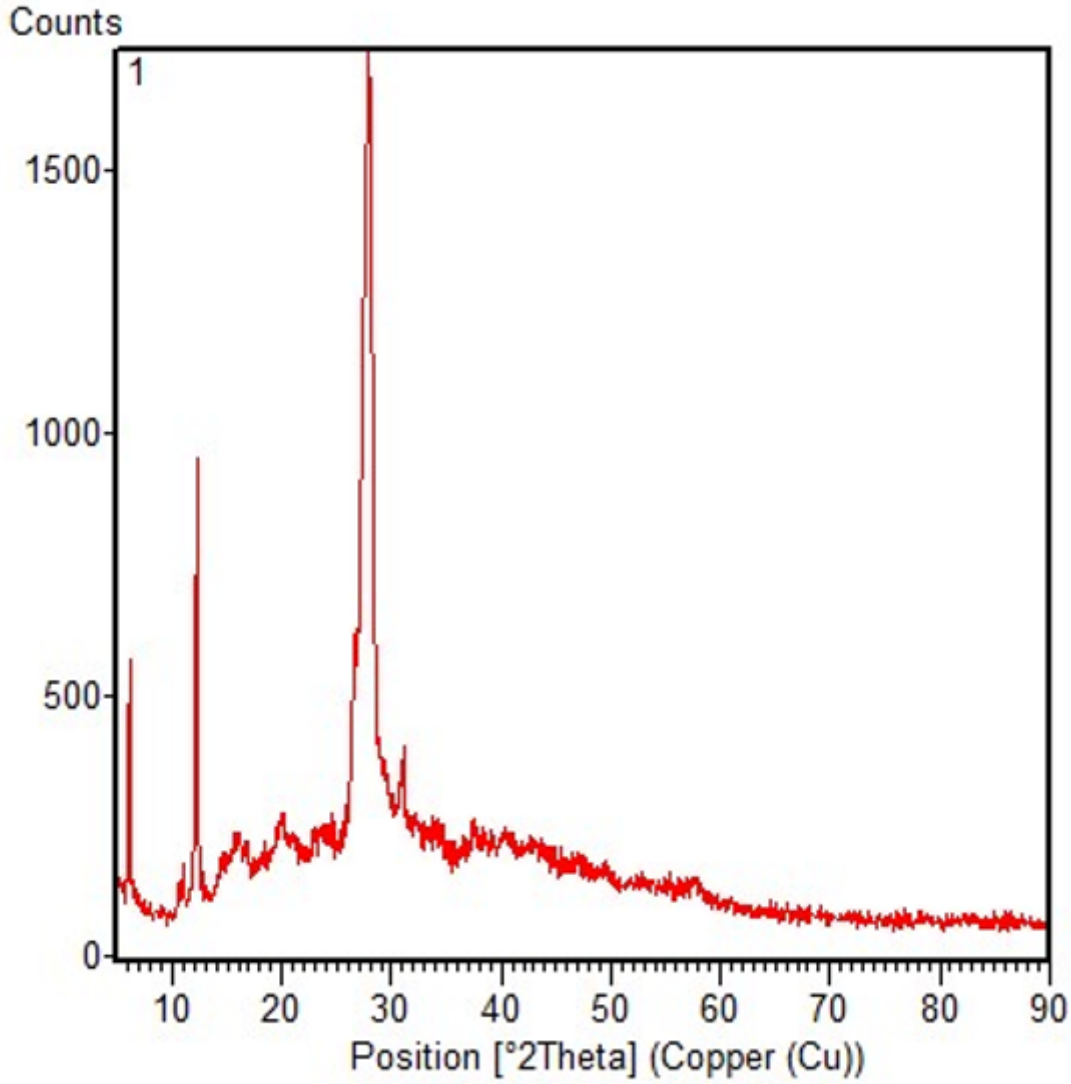

Figure 3

XRD pattern of g-C3N4/ Pr/THAM nanocatalyst

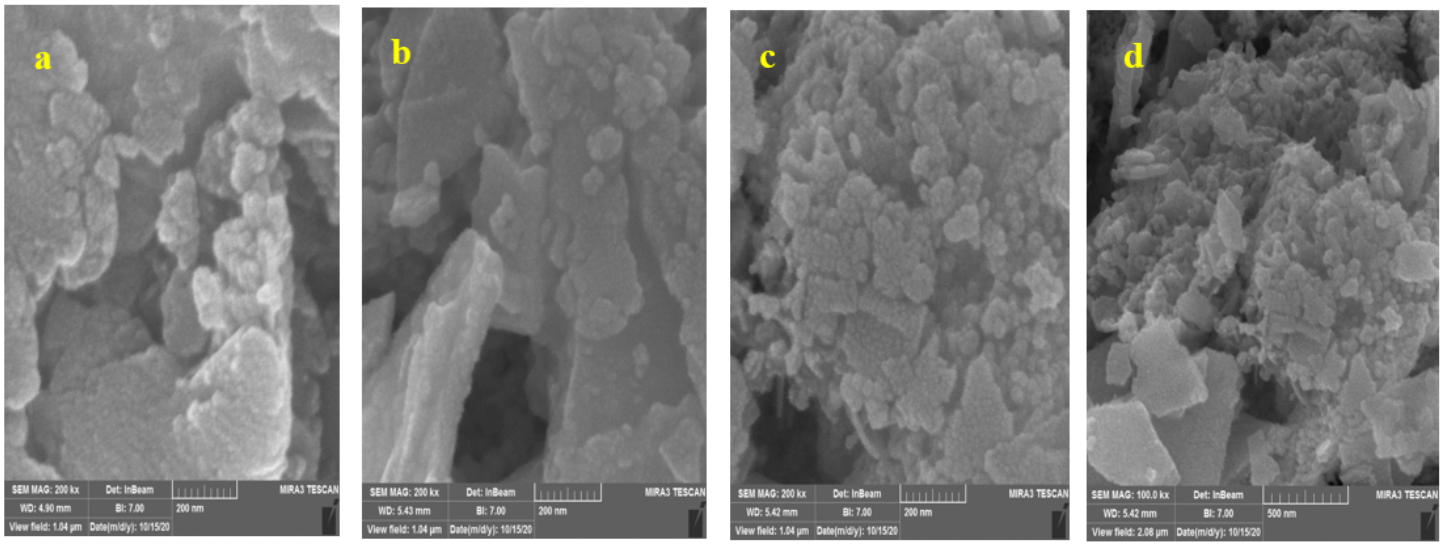

Figure 4

FESEM (a,b) images of nanosheets g-C3N4 and (c,d) images of g-C3N4/ Pr/THAM nanocatalysts.

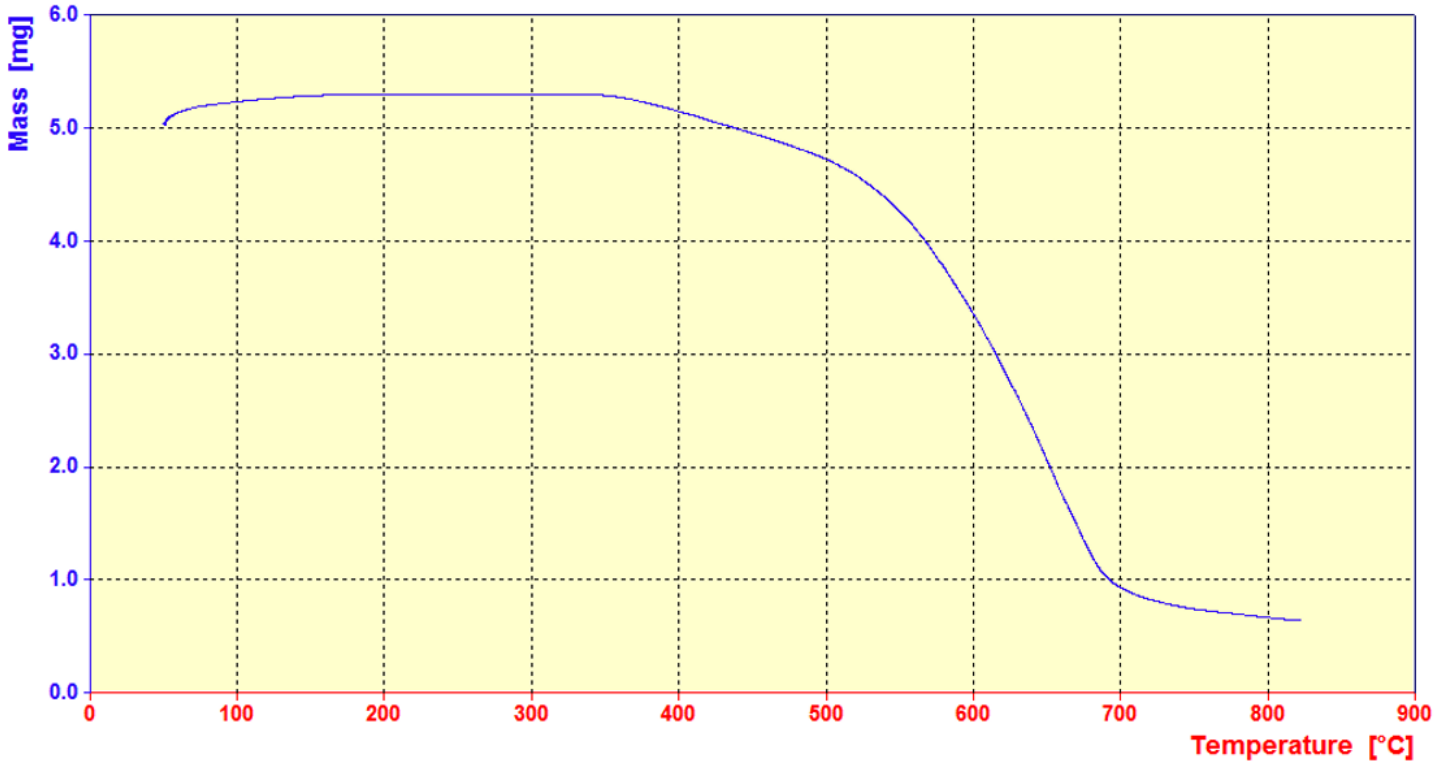

Figure 5

TGA analysis of g-C3N4/Pr/ THAM nanocatalysts

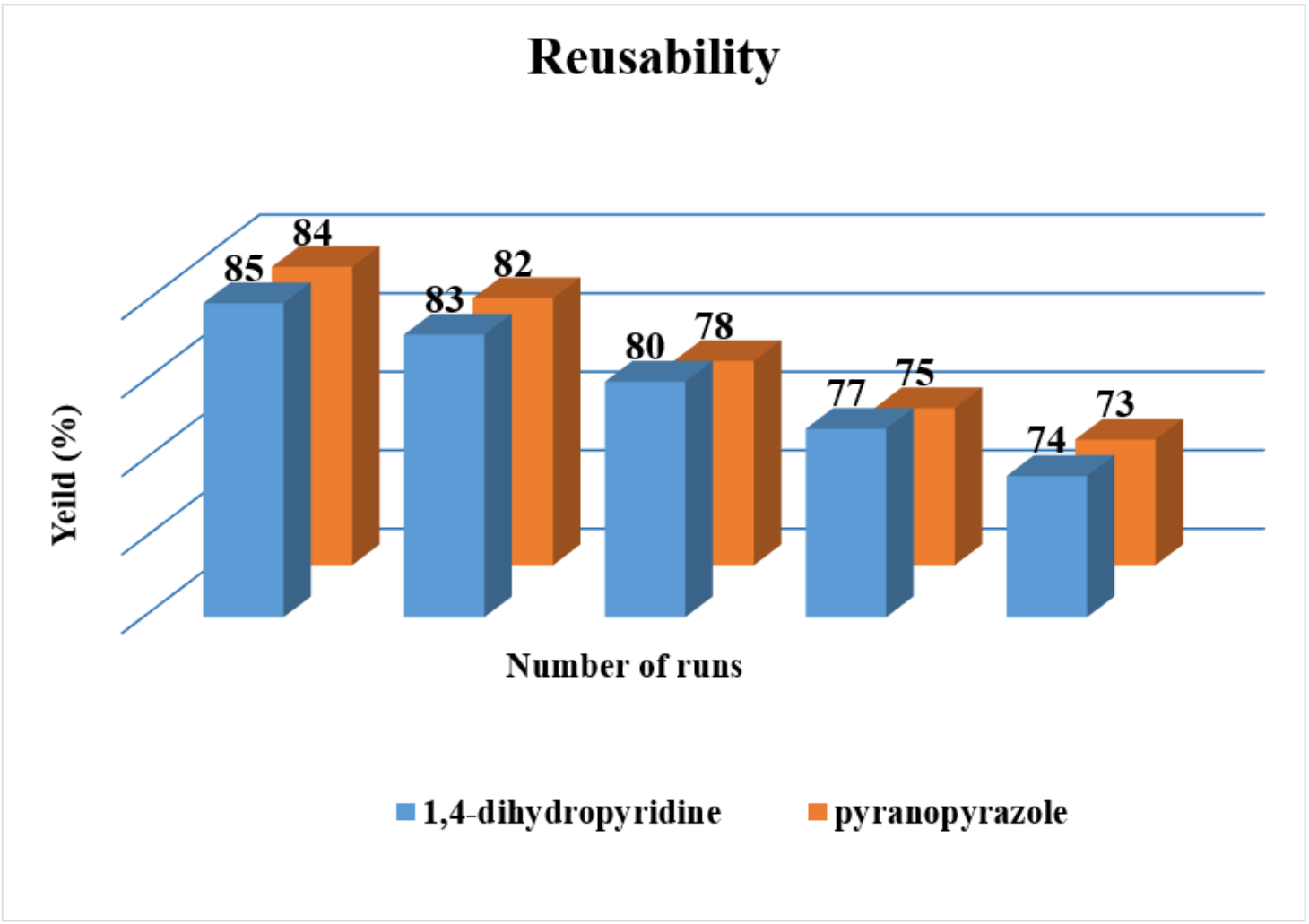

Figure 6

Reusability of the g-C3N4/Pr/ THAM nanocatalyst in the synthesis of 1,4-dihydropyridine 10 b and pyranopyrazole 5 b.

Supplementary Files

This is a list of supplementary files associated with this preprint. Click to download.

- schema1.png
- schema2.png
- schema3.png
- schema4.png